Heterogeneous Catalysis

Deutsche Ausgabe: DOI: 10.1002/ange.201601282
Internationale Ausgabe: DOI: 10.1002/anie.201601282

Controllable Hydrocarbon Formation from the Electrochemical Reduction of CO_2 over Cu Nanowire Arrays

*Ming Ma, Kristina Djanashvili, and Wilson A. Smith**

Abstract: *In this work, the effect of Cu nanowire morphology on the selective electrocatalytic reduction of CO_2 is presented. Cu nanowire arrays were prepared through a two-step synthesis of $Cu(OH)_2$ and CuO nanowire arrays on Cu foil substrates and a subsequent electrochemical reduction of the CuO nanowire arrays to Cu nanowire arrays. By this simple synthesis method, Cu nanowire array electrodes with different length and density were able to be controllably synthesized. We show that the selectivity for hydrocarbons (ethylene, n-propanol, ethane, and ethanol) on Cu nanowire array electrodes at a fixed potential can be tuned by systematically altering the Cu nanowire length and density. The nanowire morphology effect is linked to the increased local pH in the Cu nanowire arrays and a reaction scheme detailing the local pH-induced formation of C_2 products is also presented by a preferred CO dimerization pathway.*

The electrochemical reduction of CO_2 to fuel by using renewable energy has attracted considerable attention for closing the anthropogenic carbon cycle.[1–6] From electroreduction of CO_2, the captured CO_2 at the large emission sources could be used as a sustainable feedstock to be electrochemically reduced to high energy density hydrocarbons (such as CH_4 and C_2H_4).[6–9] Hydrocarbon products can be conveniently used as fuels within the existing energy infrastructure.[7] For achieving this goal, it is critical to develop a stable and cost-effective catalyst with high selectivity and efficiency. Researchers have identified various electrocatalyst materials that are capable of reducing CO_2 electrochemically in CO_2-saturated aqueous solutions.[6–14] Among currently identified catalyst materials, Cu is the only known material that is capable of catalyzing the formation of significant amounts of hydrocarbons at high reaction rates in CO_2-saturated aqueous solutions at ambient temperature and pressure.[8,10] However, controlling the selectivity of the catalytic reduction of CO_2 to a desired hydrocarbon product on a Cu catalyst remains a significant scientific challenge.

The electrochemical reduction of CO_2 to hydrocarbons on Cu catalysts is a complex process with many adsorbed intermediates (such as CO and COH) that could influence the formation of final products.[11,15] One of the important parameters in the electroreduction of CO_2 is the pH that is related to the formation of intermediates in certain reaction pathways, which could have a significant effect on products formation. The effect of local pH at the electrode/electrolyte interface on the selectivity of hydrocarbon products in the electroreduction of CO_2 was proposed by Hori in 1989,[16] showing that a locally high pH formed near Cu electrodes could facilitate the reduction of the intermediate CO to C_2H_4 and alcohols. Recently, Koper et al.[17–19] demonstrated that the electrolyte pH could play a key role in the product selectivity towards different hydrocarbons and proposed a CO coupling mechanism, indicating that C_2H_4 could be formed from a CO dimer adsorbed on Cu catalysts. Furthermore, Mul et al. reported that the formation of C_2H_4 from a CO coupling mechanism is favorable at a high local pH.[20]

Recently, we showed that CuO-derived Cu nanowire (NW) array electrodes are capable of reducing CO_2 to CO at a moderate overpotentials.[21] At more negative potentials, hydrocarbon gas phase products on Cu NW arrays were observed.[21] In this work, we tailor the selectivity of hydrocarbon products on Cu NW arrays by systematically varying the length and density of the Cu NWs which can offer a high local pH within the NW arrays. In addition, this study provides further insight into the mechanism of the hydrocarbon formation due to the enhanced CO dimerization afforded by the NW morphology.

$Cu(OH)_2$ NWs were first synthesized on Cu foils by immersing Cu foils into a solution mixture containing 0.133 M $(NH_3)_2S_2O_8$ and 2.667 M NaOH.[22,23] The increased length of $Cu(OH)_2$ NWs was obtained by immersing Cu foils in the solution mixture for longer time. After a discrete synthesis time, the Cu foils were taken out from the solution, rinsed with de-ionized water and absolute ethanol, and dried with nitrogen. CuO NWs were then fabricated by annealing the $Cu(OH)_2$ NW arrays at 150 °C for 2 hours in air.[21] The resulting CuO NW arrays were directly used in the electroreduction of CO_2, and were electrochemically reduced to Cu NW arrays during electrolysis.[21] Thus, the annealed $Cu(OH)_2$ NWs with gradually increased length and density were electrochemically reduced to Cu NWs with corresponding increased length and density.

Figure 1 shows typical SEM images of $Cu(OH)_2$ NW arrays synthesized under different synthesis time. The corresponding length of $Cu(OH)_2$ NWs prepared at different synthesis time were characterized by SEM (see Figure S4 in the Supporting Information), and the NW length as a function of synthesis time is shown in Table S1. The increase of NW length follows an enhanced NW density with increasing

[*] M. Ma, Dr. W. A. Smith
Materials for Energy Conversion and Storage (MECS), Department of Chemical Engineering, Delft University of Technology
P.O. Box 5045, 2600 GA Delft (The Netherlands)
E-mail: W.Smith@tudelft.nl
Dr. K. Djanashvili
Department of Biotechnology, Delft University of Technology
P.O. Box 5045, 2600 GA Delft (The Netherlands)

Supporting information for this article can be found under: http://dx.doi.org/10.1002/anie.201601282.

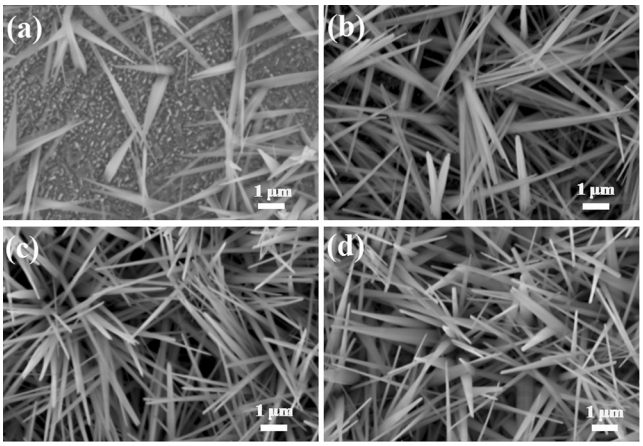

Figure 1. SEM images (a–d) of $Cu(OH)_2$ nanowires with synthesis time of 1, 3, 5, and 8 minutes, respectively.

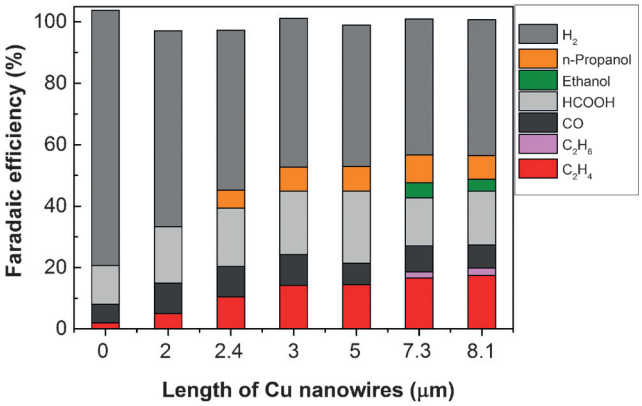

Figure 2. Faradaic efficiency for C_2H_4, C_2H_6, CO, HCOOH, ethanol, n-propanol, and H_2 on Cu nanowire arrays with different lengths at −1.1 V versus RHE in CO_2-saturated 0.1 M $KHCO_3$ electrolytes (0 μm nanowire represents Cu foil).

synthesis time (Figure S7). For simplification, the change of overall morphology as a function of synthesis time is expressed by using "nanowire length" in this study.

The electrocatalytic reduction of CO_2 on Cu NWs with different lengths was measured at −1.1 V versus the reversible hydrogen electrode (RHE) for 5 h in CO_2-saturated 0.1M $KHCO_3$ (99.95%) electrolytes (pH 6.83) at ambient temperature and pressure. CO_2 electrolysis experiments were performed in an electrochemical cell (Figure S1) consisting of working and counter electrode compartments, separated by a Nafion-115 proton exchange membrane to prevent the oxidation of CO_2 reduction products. The cathodic compartment was continuously purged with a constant CO_2 flow rate and vented directly into the gas-sampling loop of a gas chromatograph (GC) in order to enable periodic quantification of the gas-phase products. Liquid products formed during the CO_2 reduction were identified and quantified by nuclear magnetic resonance (NMR) after completion of the electrolysis experiments.

The untreated polycrystalline Cu electrodes (i.e. with no NWs) had an obvious decrease in geometric current density (j_{tot}) with a faradaic efficiency (FE) for C_2H_4 that declined from 2% at the start of electrolysis to 0% during electrolysis (Figure S8). In contrast, Cu NW arrays exhibited an initially high j_{tot} (< 3 minutes) as the CuO NWs were reduced to Cu NWs, and subsequently a stable j_{tot} was observed over electrolysis of 5 h (Figure S8).

The faradaic efficiency of products in the electrocatalytic CO_2 reduction reaction as a function of Cu NW length is presented in Figure 2. It is well-established that H_2 evolution is a competing reaction with CO_2 reduction in CO_2-saturated electrolytes, therefore the production of H_2 was also measured during electrolysis. We found that as the Cu NW arrays grew longer and more dense, the FE for H_2 production steadily decreased as the amount of CO_2 reduction products increased. In addition, the FE for C_2H_4 gradually increased with increasing the length of Cu NWs, as shown in Figure 2. Notably, the peak FE for C_2H_4 on 8.1-μm-length Cu NW arrays was maintained at 17.4% throughout the electrolysis (Figure S8), implying not only enhanced selectivity for C_2H_4 formation but also the stable catalytic activity for CO_2 reduction on Cu NWs. As we note in Figure 2, while HCOOH formation was observed on all different length of Cu NWs, n-propanol was detected on Cu catalysts with NW length greater or equal to 2.4 ± 0.56 μm. With further increasing the length of Cu NWs, C_2H_6 formation (FE = 2%) was observed, accompanying with the formation of ethanol. All the above findings indicate that the selectivity for electrochemical reduction of CO_2 to hydrocarbons can be tuned on Cu NW arrays by varying the Cu NW length and density.

In order to understand the products distribution as a function of Cu NW length, a local pH effect is proposed. It is known that the pH rises locally at the electrode/electrolyte interface due to OH^- generation in the cathodic reactions [Eqs. S(1–4)].[16] Thus, the local pH value close to the electrode becomes higher than the bulk pH.[11,16] However, HCO_3^- can neutralize the OH^- due to the reaction: $HCO_3^- + OH^- = CO_3^{2-} + H_2O$.[16] In this study, the increase of NW length also corresponds to an enhanced NW density with increasing synthesis time of the NWs (Figure S7). Thus, Cu NW arrays with an increase in nanowire length and density may cause a decrease in the diffusion of HCO_3^- into the Cu NW arrays and the diffusion of generated OH^- out of the Cu NW arrays, as shown in Figure 3a. This limitation of the diffusion process means a decreased amount of the neutralization reaction for OH^- generated near the catalyst surface, resulting in a higher local pH within the Cu NW arrays with increasing NW length and density.

To provide evidence of the local pH effect, CO_2 reduction was performed on 8.1-μm-length Cu NWs in 0.1M K_2HPO_4, 0.1M $KHCO_3$ and 0.1M $KClO_4$ electrolytes, as shown in Figure 3b. These three electrolytes were chosen due to the difference in their buffer ability. The buffer action of CO_2-saturated 0.1M K_2HPO_4 can easily neutralize OH^-, keeping the local pH at a relatively low value. While HCO_3^- can neutralize the OH^-,[16] the buffer action of HCO_3^- is weaker than the previous one. ClO_4^- does not have any buffer ability, leading to a high local pH. In this study, the diffusion ability of the three different anionic species into the NW arrays is

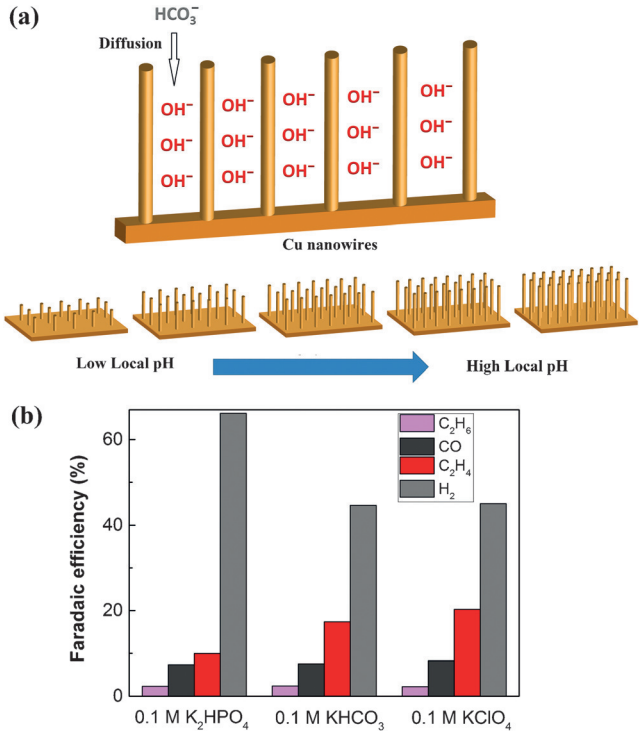

Figure 3. a) Schematic illustration of the diffusion of electrolytes into Cu nanowire arrays. b) Faradaic efficiency for C_2H_4, C_2H_6, CO and H_2 on Cu nanowire arrays (8.1 ± 1.3 μm) at −1.1 V versus RHE in CO_2-saturated 0.1 M K_2HPO_4 (pH 6.5), CO_2-saturated 0.1 M $KHCO_3$ (pH 6.8) and CO_2-saturated 0.1 M $KClO_4$ (pH 5.9) electrolytes, respectively.

considered to be identical due to the same concentration of anionic species (0.1M). Thus, the local pH at the electrode/electrolyte interface could be affected by the buffer ability of different electrolytes for Cu NWs (i.e. the local pH can be estimated as: $KClO_4 > KHCO_3 > K_2HPO_4$).

We found that the product distribution on Cu NWs was significantly influenced by the different electrolytes. H_2 evolution (FE = 66%) was dramatically promoted in K_2HPO_4 electrolytes with suppressed CO_2 reduction, in contrast, $KHCO_3$ and $KClO_4$ solutions favored CO_2 reduction with a reduced FE for H_2 evolution. In addition, the FE of CO and C_2H_6 were roughly equal in the three different electrolytes. Interestingly, while the enhanced FE of 17.4% for C_2H_4 (FE for C_2H_4 is 10% in 0.1M K_2HPO_4) was observed in 0.1M $KHCO_3$, the highest FE of 20.3% for C_2H_4 was obtained in 0.1M $KClO_4$ solutions (Figure 3b). Furthermore, the highest and lowest FE for ethanol formation were discovered in 0.1M $KClO_4$ and 0.1M K_2HPO_4, respectively (Figure S11). These observations (FE for C_2H_4 and ethanol: $KClO_4 > KHCO_3 > K_2HPO_4$) are consistent with previous studies on the Cu foil electrodes reported by Hori.[11,16] Thus, a locally high pH formed at Cu catalysts could favor the formation of C_2H_4 and alcohols. In addition, the low pH value at the electrode/electrolyte interface favors H_2 evolution.[11] We therefore conclude the enhanced selectivity for C_2H_4 with suppressed H_2 evolution on the longer and more dense Cu NW arrays is attributed to the high local pH formed in the Cu NW arrays (Figure 3a). In addition, the enhanced local pH on Cu NWs may contribute to the observed ethanol formation on the longer Cu NW length ($\geq 7.3 \pm 1.3$ μm)

To gain further insight into the mechanism of the products distribution on Cu NW arrays, we propose a reaction pathway for electrocatalytic CO_2 reduction, as shown in Scheme 1. It is

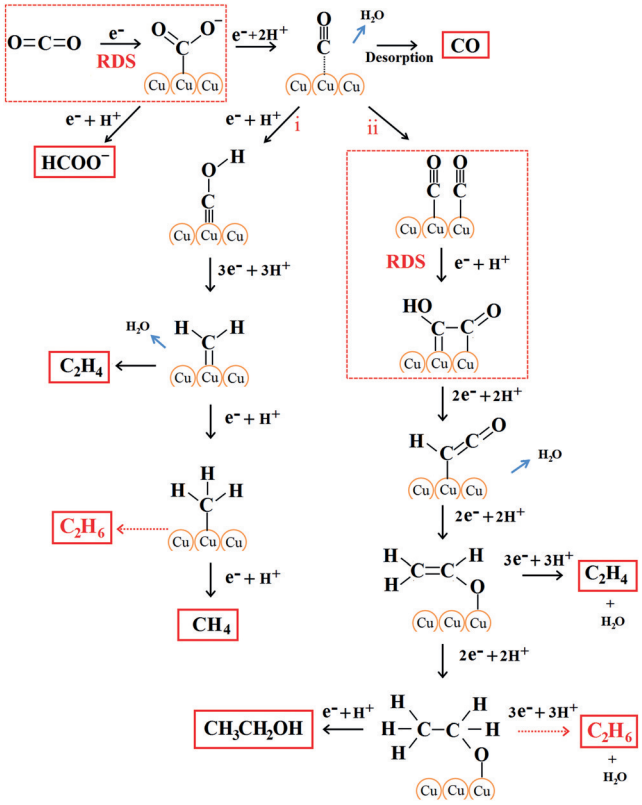

Scheme 1. Proposed reaction paths for electrocatalytic reduction of CO_2 on Cu nanowire arrays, with path (i), left, showing COH formation, and path (ii), right, showing CO dimerization. In path (i), $2CH_2$ and $2CH_3$ intermediates are required for C_2H_4 and C_2H_6 formation, respectively.

generally accepted that CO is a key intermediate for the formation of hydrocarbons in the electrochemical reduction of CO_2.[11,24] However, it is generally accepted that the first electron transfer for the formation of the $CO_2^{\bullet-}$ shown in Scheme 1 is the rate determining step (RDS) in the electrochemical reduction of CO_2 to CO because the first electron transfer requires a much more negative potential compared to the following steps.[25] We have previously reported the enhanced stabilization for the $CO_2^{\bullet-}$ intermediate on Cu NW arrays.[21] The more active sites that are provided by longer Cu NWs may lead to the enhanced stabilization of the $CO_2^{\bullet-}$. In addition, the suppressed CO_2 reduction with enhanced H_2 evolution at low local pH caused by strong buffer action of K_2HPO_4 electrolytes (Figure 3b) may indicate the local pH formed in the Cu NW arrays may play a significant role in the CO_2 activation.

Furthermore, the FE of products as a function of potential was plotted for 8.1-μm-length Cu NWs (Figure 4a). We found that the FE for CO decreased from −0.7 V to −1.1 V versus RHE, along with enhanced FE for C_2H_6 and C_2H_4. In

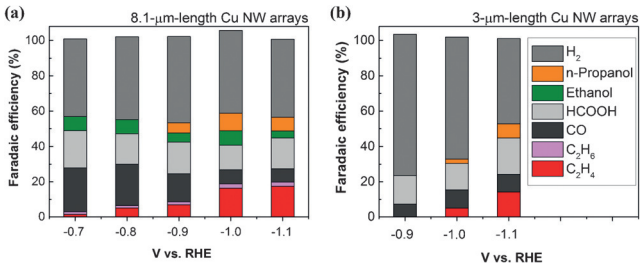

Figure 4. Faradaic efficiency of the products at various potentials in CO_2-saturated 0.1 M $KHCO_3$.

addition, the n-propanol was detected at potentials lower or equal to −0.9 V. These observations imply that the formation of hydrocarbons from the CO intermediate is more favorable at more negative potentials.

It was reported that one possible reaction path for C_2H_4 formation is through a CH_2 dimerization.[10] Furthermore, more detailed reaction pathway for C_2H_4 has been investigated theoretically by density functional theory (DFT), which provides a pathway through a COH intermediate shown in Scheme 1 (path i, left).[26] Recently, a CO coupling mechanism[18,19,24] has been suggested as an alternative route to C_2H_4 through a CO dimer adsorbed on Cu, as shown in Scheme 1 (path ii, right). Thus, C_2H_4 formation could have two potential pathways, (i) through a COH intermediate and (ii) through a CO dimerization pathway. It is critical to understand which pathway is preferred for the Cu NW arrays to determine the mechanism of the selectivity for hydrocarbons. When comparing the two pathways, it can be seen that CH_4 is only formed through the COH intermediate pathway (path i). In all our experiments, C_2H_4 was observed without any detected CH_4 formation, which may indicate that C_2H_4 formation on Cu NWs is mainly from the CO dimerization reaction path (path ii).

In addition, the formation of C_2H_6 has not been reported in the electrocatalytic reduction of CO_2 on smooth Cu,[7,8,11] but was observed as a minor product on nanostructured Cu catalysts.[3,27,28] However, a reaction pathway towards C_2H_6 has never been reported. Here we propose two possible routes for C_2H_6 formation via CH_3 dimerization and CH_3CH_2O intermediate in Scheme 1. In our research, C_2H_6 formation appeared on longer Cu NWs (NW $\geq 7.3 \pm 1.3$ μm), and was always accompanied with the formation of ethanol without any observed CH_4 formation (Figure 2), which implies that C_2H_6 and ethanol may be formed through the same intermediate (CH_3CH_2O) in the CO dimerization pathway,[18] as we proposed in Scheme 1.

As discussed above, the formation of C_2H_4, C_2H_6 and ethanol could be mainly from the CO dimerization reaction pathway in this study. The rate determining step for the formation of C_2H_4 in the CO dimerization pathway is CO coupling (Scheme 1).[24] It has been demonstrated that the CO coupling step is favored at a high local pH near the catalyst surface.[20] In addition, more products (such as C_2H_6 and ethanol) are detected on longer Cu NW arrays at various potentials shown in Figure 4, indicating that the enhanced local pH on Cu NWs may contribute to the observation of C_2H_6 and ethanol. Therefore, the higher local pH in the Cu NW arrays with an increase in nanowire length and density could improve the formation of C_2H_4, C_2H_6 and ethanol through the enhanced CO coupling mechanism which is formed in a high local pH due to the nanowire morphology.

In summary, the effect of Cu nanowire morphology has been explored for the electrochemical reduction of CO_2. With increasing the Cu nanowire length ($\geq 2.4 \pm 0.56$ μm), the formation of n-propanol was detected along with CO, HCOOH and C_2H_4. Furthermore, C_2H_6 formation appeared on longer Cu nanowires ($\geq 7.3 \pm 1.3$ μm), accompanying with the formation of ethanol. We propose a route to C_2H_6 from the intermediate (CH_3CH_2O) in the CO dimerization pathway. More importantly, Cu nanowire arrays exhibited an increased selectivity for C_2H_4 with increasing the Cu nanowire length and density, which is ascribed to the improved formation of C_2H_4 through a CO coupling mechanism caused by an enhanced local pH in the Cu nanowire arrays. This study shows that the selectivity in the electrocatalytic reduction of CO_2 to hydrocarbons could be tuned on Cu nanowire arrays by varying the Cu nanowire length, providing a promising efficient approach for systematically controlling hydrocarbon formation through the electrochemical reduction of CO_2.

Acknowledgements

This work is supported by the Chinese Scholarship Council, and the NWO VENI grant awarded to W.A.S.. The authors would like to thank Prof. Bernard Dam, Dr. David Vermaas, Dr. Francesc Sastre, and Moreno de Respinis for helpful discussions.

Keywords: carbon dioxide · CO_2 conversion · electrocatalysis · heterogeneous catalysis · nanowires

How to cite: *Angew. Chem. Int. Ed.* **2016**, *55*, 6680–6684
Angew. Chem. **2016**, *128*, 6792–6796

[1] D. T. Whipple, P. J. A. Kenis, *J. Phys. Chem. Lett.* **2010**, *1*, 3451–3458.
[2] J. L. DiMeglio, J. Rosenthal, *J. Am. Chem. Soc.* **2013**, *135*, 8798–8801.
[3] C. W. Li, M. W. Kanan, *J. Am. Chem. Soc.* **2012**, *134*, 7231–7234.
[4] Y. Chen, C. W. Li, M. W. Kanan, *J. Am. Chem. Soc.* **2012**, *134*, 19969–19972.
[5] Y. Chen, M. W. Kanan, *J. Am. Chem. Soc.* **2012**, *134*, 1986–1989.
[6] J. Qiao, Y. Liu, F. Hong, J. Zhang, *Chem. Soc. Rev.* **2014**, *43*, 631–675.
[7] M. Gattrell, N. Gupta, A. Co, *J. Electroanal. Chem.* **2006**, *594*, 1–19.
[8] K. P. Kuhl, E. R. Cave, D. N. Abram, T. F. Jaramillo, *Energy Environ. Sci.* **2012**, *5*, 7050–7059.
[9] K. Manthiram, B. J. Beberwyck, A. P. Alivisatos, *J. Am. Chem. Soc.* **2014**, *136*, 13319–13325.
[10] Y. Hori, R. Takahashi, Y. Yoshinami, A. Murata, *J. Phys. Chem. B* **1997**, *101*, 7075–7081.
[11] Y. Hori in *Modern Aspects of Electrochemistry, Vol. 42* (Eds: C. G. Vayenas, R. E. White, M. E. Gamboa-Aldeco), Springer, New York, **2008**, pp. 89–189.

[12] S. Zhang, P. Kang, S. Ubnoske, M. K. Brennaman, N. Song, R. L. House, J. T. Glass, T. J. Meyer, *J. Am. Chem. Soc.* **2014**, *136*, 7845 – 7848.
[13] S. Zhang, P. Kang, T. J. Meyer, *J. Am. Chem. Soc.* **2014**, *136*, 1734 – 1737.
[14] H.-E. Lee, K. D. Yang, S. M. Yoon, H.-Y. Ahn, Y. Y. Lee, H. Chang, D. H. Jeong, Y.-S. Lee, M. Y. Kim, K. T. Nam, *ACS Nano* **2015**, *9*, 8384 – 8393.
[15] A. A. Peterson, J. K. Nørskov, *J. Phys. Chem. Lett.* **2012**, *3*, 251 – 258.
[16] Y. Hori, A. Murata, R. Takahashi, *J. Chem. Soc. Faraday Trans. 1* **1989**, *85*, 2309.
[17] K. J. P. Schouten, Z. Qin, E. Pérez Gallent, M. T. M. Koper, *J. Am. Chem. Soc.* **2012**, *134*, 9864 – 9867.
[18] F. Calle-Vallejo, M. T. M. Koper, *Angew. Chem. Int. Ed.* **2013**, *52*, 7282 – 7285; *Angew. Chem.* **2013**, *125*, 7423 – 7426.
[19] K. J. P. Schouten, E. Pérez Gallent, M. T. M. Koper, *J. Electroanal. Chem.* **2014**, *716*, 53 – 57.
[20] R. Kas, R. Kortlever, H. Yılmaz, M. T. M. Koper, G. Mul, *ChemElectroChem* **2015**, *2*, 354 – 358.
[21] M. Ma, K. Djanashvili, W. A. Smith, *Phys. Chem. Chem. Phys.* **2015**, *17*, 20861 – 20867.
[22] W. Zhang, X. Wen, S. Yang, Y. Berta, Z. L. Wang, *Adv. Mater.* **2003**, *15*, 822 – 825.
[23] C. Lin, Y. Lai, D. Mersch, E. Reisner, *Chem. Sci.* **2012**, *3*, 3482 – 3487.
[24] K. J. P. Schouten, Y. Kwon, C. J. M. van der Ham, Z. Qin, M. T. M. Koper, *Chem. Sci.* **2011**, *2*, 1902.
[25] Q. Lu, J. Rosen, Y. Zhou, G. S. Hutchings, Y. C. Kimmel, J. G. Chen, F. Jiao, *Nat. Commun.* **2014**, *5*, 3242.
[26] X. Nie, M. R. Esopi, M. J. Janik, A. Asthagiri, *Angew. Chem. Int. Ed.* **2013**, *52*, 2459 – 2462; *Angew. Chem.* **2013**, *125*, 2519 – 2522.
[27] W. Tang, A. Peterson, A. S. Varela, Z. P. Jovanov, L. Bech, W. J. Durand, S. Dahl, J. K. Nørskov, I. Chorkendorff, *Phys. Chem. Chem. Phys.* **2012**, *14*, 76 – 81.
[28] S. Sen, D. Liu, G. T. R. Palmore, *ACS Catal.* **2014**, *4*, 3091 – 3095.

Received: February 4, 2016
Published online: April 21, 2016

